Microstructure Evolution of Cu-15Ni-8Sn Alloy Prepared by Vertical Semi-continuous Casting with EMS

Zhongkai Guo[1], Jinchuan Jie[1]*, Shipeng Yue[1], Tingju Li[1], Qingtao Guo[2]

[1]Key Laboratory of Solidification Control and Digital Preparation Technology(Liaoning Province), School of Material Science and Engineering, Dalian University of Technology, Dalian 116024, Liaoning, China
[2]State Key Laboratory of Metal Material for Marine Equipment and Application, Anshan, 114000, China

[*]*Corresponding author: jiejc@dlut.edu.cn*

Abstract
In the present study, vertical semi-continuous casting equipped with the electromagnetic stirring (EMS) was applied in order to control the solidification process and obtain the anticipated homogeneous microstructure for Cu-15Ni-8Sn alloy. The experimental results indicate that the microstructure of as-cast Cu-15Ni-8Sn (wt.%) alloy prepared by conventional casting consists of Sn-depleted α phase (α Cu(Ni) solid solution), Sn-rich γ phase ($(Cu_xNi_{1-x})_3Sn$), and intermediate transition region (α+γ), and most of the Sn element mainly segregates at dendritic grain boundary. Discriminatively, some equiaxed grains come into being in as-cast Cu-15Ni-8Sn alloy prepared by vertical semi-continuous casting, and Sn-rich γ phases distribute on the matrix and grain boundary uniformly. Furthermore, the size of equiaxed grains becomes smaller after applying EMS, which reduces the segregation of Sn element to a large degree. In this study, microstructure evolution mechanism of Cu-15Ni-8Sn alloy prepared by conventional casting and by vertical semi-continuous casting without and with EMS is analyzed.

Keywords: Cu-15Ni-8Sn, Vertical semi-continuous casting, Electromagnetic stirring, Microstructure evolution

1. Introduction
A commercial Cu-Ni-Sn alloy, strengthened by spinodal decomposition [1], is widely used in electronic industry, aerospace, mechanical systems and so on due to its high strength, high elastic, good mechanical properties, and electrical conductivity, etc [2-6]. However, some previous studies [3, 4] indicate that a serious segregation phenomenon of Sn element exists in the conventional casting process for Cu-Ni-Sn alloy as a result of the low-melting-point of Sn compared to Cu and Ni, which has a negative influence on the subsequent processing and mechanical properties. Therefore, in recent decades, great efforts have been carried out to explore for new preparation technology such as powder metallurgy [7], rapid solidification [8, 9], spray deposition [10] and so on to reduce the segregation of Sn. Although Cu-Ni-Sn alloy has been successfully prepared by such above-mentioned methods, it should be noted that the high cost and small size limitation of samples via such complex preparation process have become to the great obstacles for industrial production and application.

Therefore, the industrial production and application of Cu-Ni-Sn alloy become increasingly significant. Grain refinement is one of the alternative means to reduce the segregation. Grain refinement can be achieved by several methods, i.e., (a) the addition of grain refiner in aluminum alloys [11]; (b) the stirring of melt by mechanical equipment or electromagnetic field [12-14]. In the present study, vertical semi-continuous casting equipped with electromagnetic stirring (EMS) is applied for the industrial production of Cu-15Ni-8Sn alloy to reduce the segregation of Sn. The microstructure evolution mechanism of Cu-15Ni-8Sn alloy prepared by conventional casting and by vertical semi-continuous casting without and with EMS is analyzed. The results provide a fundamental understanding for the industrial preparation of Cu-Ni-Sn alloy, which has tremendous scientific and technological relevance.

2. Experimental
2.1 Preparation of Cu-15Ni-8Sn alloy
Cu-15Ni-8Sn (wt%) alloy billet (the cross section is 100 mm × 100 mm, the length is 500 mm) was prepared by vertical semi-continuous casting with EMS using an intermediate frequency induction furnace. The raw materials are electrolytic copper plate (99.95 wt.%), electrolytic nickel plate (99.95 wt.%) and industrial pure tin (99.95 wt.%). Industrial pure tin was added into the furnace after the electrolytic copper and electrolytic nickel were completely melting, then the temperature was held at 1350℃ for 10 minutes to guarantee that the mixing melt was homogeneous. In order to avoid the oxidation of the melt surface, the carbon powder was used to cover the surface of the alloy melt. Magnesium-copper master alloy was used for degassing in the casting process. Then, the melt was poured into a crystallizer with a vibration equipment and an intermediate frequency induction coil. The coil was superimposed on a certain height of the crystallizer where the solid-liquid interface was located exactly at the height. The schematic diagram of experiment device is shown in Fig.1. The power of the intermediate frequency magnetic field are 0 KW, 5 KW, 10 KW, respectively. In addition, as a comparison experiment, the Cu-15Ni-8Sn

alloy ingot (the diameter is 40mm, the length is 200mm) was prepared by using an intermediate frequency induction furnace under argon atmosphere.

2.2 Microstructure observation and phase identification

In order to analyze the solidification behavior of Cu-15Ni-8Sn alloy, the as-obtained samples were polished and etched by a solution consisting of 95 ml C_2H_5OH + 5 ml HCl + 5 g $FeCl_3$ for morphology observation and phase identification. Microstructure was observed using an Olympus GX51 optical microscope and a scanning electron microscope (SEM, Zeiss supra 55) equipped with an energy dispersive spectrometer (EDS) operated in secondary electron mode and with an accelerating voltage of 15 kV.

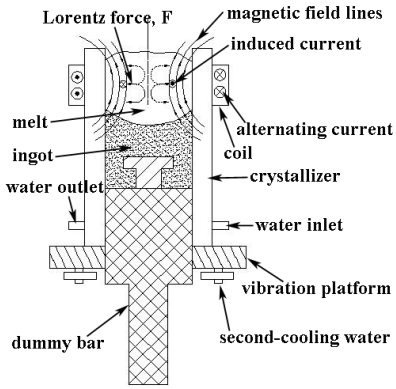

Fig. 1 The schematic diagram of experiment device

3. Results and discussion

3.1 Microstructure of as-cast Cu-15Ni-8Sn alloy prepared by conventional casting

Fig. 2 shows the microstructure of as-cast Cu-15Ni-8Sn alloy prepared by conventional casting. It can be clearly seen that the developed dendritic microstructure which exhibits various growth orientations exists in as-cast Cu-15Ni-8Sn alloy as shown in Fig. 2(a). The dark grey phase relates to matrix and the light grey phase corresponds to dendritic grain boundary. Most of Sn element segregates at the dendritic grain boundary which presents a width of hundreds of micrometers. The dendritic matrix consists of Sn-depleted α matrix, nubby Sn-rich γ phase, and slight intermediate transition region as indicated by Fig. 2(b). There are some nubby Sn-rich γ phases located at dendritic grain boundary as shown in Fig.2(c), which can be identified as $(Cu_xNi_{1-x})_3Sn$ according to the EDS result in Fig. 2(d). In addition, lamellar (α+γ) phases can also be clearly found at grain boundary, which is similar to the pearlite in steel.

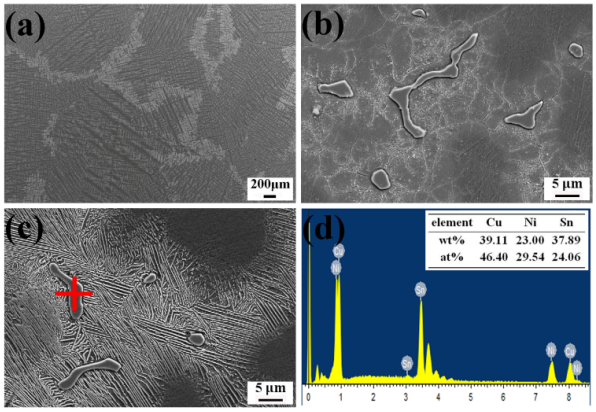

Fig. 2 (a), (b), (c) Microstructure of as-cast Cu-15Ni-8Sn alloy prepared by conventional casting; (d) the corresponding EDS result of the point in (c).

As is well known, phase diagram is an important tool for understanding and ascertaining the solidification behavior of an alloy. Fig. 3(a) shows the quasi binary phase diagram of Cu-15Ni-XSn (wt.%) calculated by CALPHAD. According to the phase diagram, the melting point of Cu-15Ni-8Sn alloy is about 1110℃, which is in agreement with that calculated by Jyrki Miettinen [15]. In addition, the temperature range of liquid-solid transformation is about 190℃ (from about 1110℃ to 920℃), which can be considered to be the main reason for

the Sn segregation. As for equilibrium simulation, the solid fraction versus temperature curve gently falls. There is only a single α Cu(Ni) phase after the solidification is completed at about 920℃. However, the small platform on Scheil simulation curve can be ascertained as the formation temperature of γ phase, which is about 830 ℃. During practical solidification process for Cu-15Ni-8Sn alloy, the firstly formed phase possesses a composition of kC_0, which is smaller than the average composition of the alloy. Consequently, the low-melting-point Sn-rich melt are pushed to dendritic boundaries, causing the segregation of Sn along grain boundaries. Most of the Sn-rich melt can solidify to supersaturated α phase, and only a few fraction of Sn-rich melt forms nubby γ phases via liquid-solid transformation. Subsequently lamellar γ phase would precipitate from supersaturated α solid solution and exhibit lamellar (α+γ) phases as indicated in Fig. 2(c). In addition, there are also some Sn-rich droplets existed in dendritic matrix due to insufficient diffusion for Sn atoms. These Sn-rich droplets would solidify to γ phases at about 830 ℃ just as demonstrated in Fig. 2(b).

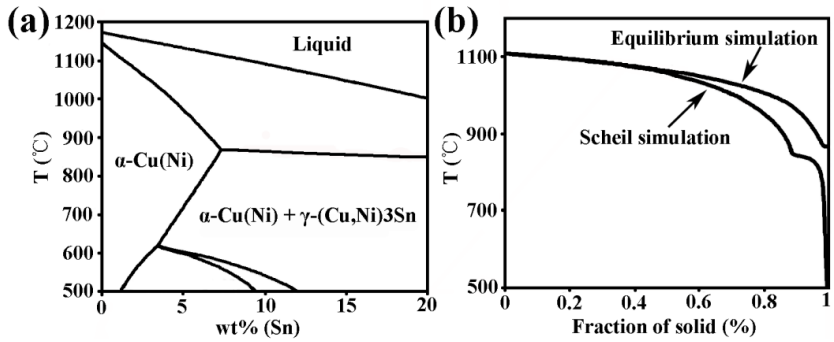

Fig. 3 (a) Quasi binary phase diagram of Cu15Ni-XSn alloy, (b) Sheil and equilibrium simulations of Cu-Ni-Sn solidification.

3.2 Microstructure of as-cast Cu-15Ni-8Sn alloy prepared by vertical semi-continuous casting without and with EMS

Fig. 4 shows microstructure of the as-cast Cu-15Ni-8Sn alloy prepared by vertical semi-continuous casting under different powers of the intermediate frequency magnetic field. Some coarse equiaxed grains come into being as shown in Fig4. (a) when the vibration caused by mechanical equipment is introduced during the casting process. The Sn-rich γ phases distribute on the matrix and grain boundary equally. Furthermore, the size of equiaxed grains becomes smaller with the increasing power of the intermediate frequency magnetic field after the EMS is applied. Especially, the size of equiaxed grains can be reduced to about 100 μm as demonstrated in Fig4. (c) when the power of the intermediate frequency magnetic field is 10 KW, which reduce the segregation of Sn to a large degree.

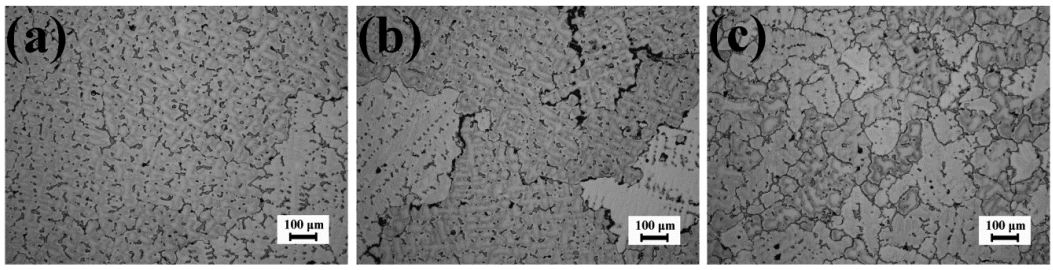

Fig. 4 Microstructures of the as-cast Cu15Ni-8Sn alloy under different powers of the intermediate frequency magnetic field: (a) 0 KW; (b) 5 KW; (c) 10 KW.

On the one hand, the vibration device of crystallizer is introduced in order to reduce the friction between the ingot surface and the wall of the crystallizer. Consequently, the ingot can be successfully prepared and the quality of the ingot surface has been improved greatly. On the other hand, the vibration of crystallizer can break up the dendrite arms and promote the formation of equiaxed grains. Moreover, the refining effect on the grain becomes more obvious after the EMS is applied. The fundamental principle of EMS is to create a Lorentz force, F, acting on the alloy melt. The alternating electromagnetic field, B, would be born when the coil is connected to an alternating current. Subsequently, the induced current, J, can be generated in the alloy melt. Lorentz force, F, can be caused by the interaction of induced current and alternating electromagnetic field. It can be given by

$$F = J \times B = \nabla(\mu B^2/2)(1/\mu) + (B \bullet \nabla)B \quad (1)$$

where the μ is the permeability. The first item on the right of the formula is the radial partial force which is vertical to the side of the melt and points to the center of the melt. The contact pressure between the melt and the wall of crystallizer can be reduced by the radial partial force, thus achieving the purpose of soft-contact electromagnetic semi-continuous casting. The second item is the cornering force caused by the edging-effect which can stir the melt by generating a vertical downward whirl. During the solidification of Cu-15Ni-8Sn alloy, dendrite arms can be fragmented by the Lorentz force and transformed through the mushy zone by forced convection. Some fragments could survive in the melt and become the cores of heterogeneous nucleation, which lead to the formation of the refined equiaxed grains. In addition, the temperature gradient could be lowered under EMS, which extends the undercooling region and contributes to the dendritic-to-equiaxed transition.

4. Conclusions:

Cu-15Ni-8Sn alloy was prepared by conventional casting and by vertical semi-continuous casting without and with EMS. The microstructure evolution mechanism is investigated in the present study. The microstructure of as-cast Cu-15Ni-8Sn alloy prepared by conventional casting consists of Sn-depleted α phase (α Cu(Ni) solid solution), Sn-rich γ phase ($(Cu_xNi_{1-x})_3Sn$), and intermediate transition region (α+γ), and most of the Sn element mainly segregates at dendritic grain boundary. Whereas, some equiaxed grains come into being in as-cast Cu-15Ni-8Sn alloy prepared by vertical semi-continuous casting, and Sn-rich γ phases distribute on the matrix and grain boundary uniformly. Furthermore, the size of equiaxed grains becomes smaller with the increasing power of the intermediate frequency magnetic field after EMS is applied, which reduces the segregation of Sn element to a large degree. The grain refinement can be ascribed to the double effects of the vibration of crystallizer and EMS. During solidification, dendrite arms can be fragmented and become the cores of heterogeneous nucleation, consequently, forming refined equiaxed grains after solidification.

Acknowledgment

The authors gratefully acknowledge the supports of National Key Research and Development Program of China (Nos. 2017YFA0403800), the National Natural Science Foundation of China (Nos. 51771040, 51690163, 51525401), State Key Laboratory of Metal Material for Marine Equipment and Application (No. SKLMEA-K201701)

References

1. L.H. Schwartz, S. Mahajan, J.T. Plewes, Acta Metallurgica, 22 (1974) 601-609.
2. W.R. Cribb, M.J. Gedeon, F.C. Grensing, Advanced Materials & Processes, 171 (2013) 20-25.
3. W.R. Cribb, F.C. Grensing, (2009).
4. W.R. Cribb, F.C. Grensing, Canadian Metallurgical Quarterly, 50 (2013) 232-239.
5. C.R. Scorey, S. Chin, M.J. White, R.J. Livak, JOM, 36 (1984) 52-54.
6. J.C. Rhu, S.K. Sang, C.J. Yun, S.Z. Han, J.K. Chang, Metallurgical & Materials Transactions A, 30 (1999) 2649-2657.
7. P. Goudeau, A. Naudon, J.M. Welter, Scripta Metallurgica, 22 (1988) 1019-1022.
8. L.E. Collins, J.R. Barry, Materials Science & Engineering, 98 (1988) 335-338.
9. L. Deyong, R. Tremblay, R. Angers, Materials Science & Engineering A, 124 (1990) 223-231.
10. R.H. Cookey, J.V. Wood, Powder Metallurgy, 33 (2013) 335-338.
11. A.L. Greer, A.M. Bunn, A. Tronche, P.V. Evans, D.J. Bristow, Acta Materialia, 48 (2000) 2823-2835.
12. T. Campanella, C. Charbon, M. Rappaz, Metallurgical & Materials Transactions A, 35 (2004) 3201-3210.
13. W.D. Griffiths, D.G. Mccartney, Materials Science & Engineering A, 216 (1996) 47-60.
14. D. Lu, Y. Jiang, G. Guan, R. Zhou, Z. Li, R. Zhou, Journal of Materials Processing Tech, 189 (2007) 13-18.
15. J. Miettinen, Calphad-computer Coupling of Phase Diagrams & Thermochemistry, 27 (2003) 309-318.